Synthesis of Crosslinked PEG/IL Blend Membrane via One-Pot Thiol–Ene/Epoxy Chemistry

Jing Deng, Zhongde Dai, Liyuan Deng

Department of Chemical Engineering, Norwegian University of Science and Technology, 7491, Trondheim, Norway
Correspondence to: L. Deng (E-mail: deng@nt.ntnu.no)

Received 18 November 2019; Revised 20 December 2019; accepted 20 December 2019
DOI: 10.1002/pol.20190195

ABSTRACT: Poly(ethylene glycol) (PEG)-based membranes have obtained considerable attentions for CO_2 separation for their promising CO_2 separation performance and excellent thermal/chemical resistance. In this work, a one-pot thiol–ene/epoxy reaction was used to prepare crosslinked PEG-based and PEG/ionic liquids (ILs) blend membranes. Four ILs of the same cation $[Bmim]^+$ with different anions ($[BF_4]^-$, $[PF_6]^-$, $[NTf_2]^-$, and $[TCM]^-$) were chosen as the additives. The chemical structure, thermal properties, hydrophilicity, and permeation performance of the resultant membranes were investigated to study the ILs' effects. An increment in CO_2 permeability (~34%) was obtained by optimizing monomer ratios and thus crosslinking network structures. Adding ILs into optimized PEG matrix shows distinct influences in CO_2 separation performance depending on the anions' types, due to the different CO_2 affinities and compatibilities with PEG matrix. Among these ILs, $[Bmim][NTf_2]$ was found the most effective in enhancing CO_2 transport by simultaneously increasing the solubility and diffusivity of CO_2. © 2020 The Authors. *Journal of Polymer Science* published by Wiley Periodicals, Inc. J. Polym. Sci. **2020**

KEYWORDS: CO_2 separation; click chemistry; epoxy resin; ionic liquids; poly(ethylene glycol)

INTRODUCTION Epoxy resins, or called polyepoxides, are a class of polymers formed by monomers or oligomers containing epoxy groups,[1] usually with the presence of crosslinkers, such as amines. The excellent chemical and thermal resistance, good mechanical properties, and notable adhesion of epoxy resins allow them to play important roles in various industrial applications, such as coating, reinforcement,[2,3] and adhesives.[4–7] Recently, several groups have expanded these materials to gas separation, especially as CO_2 separation membranes, thanks to the facile and rapid crosslinking, tunable chemical structure and the presence of secondary amines.[8–11] In addition, the used epoxy monomers are mainly focused on poly(ethylene glycol) (PEG)-based materials, which have been considered as one of the most promising materials to overcome the trade-off between gas permeability and selectivity of the polymeric membranes,[12] due to the high CO_2 solubility and solubility selectivity.[13,14]

A series of crosslinked PEG membranes based on the epoxy–amine reaction for CO_2 capture have been reported.[8,15–21] Thanks to the CO_2-philic ethylene oxide (EO) units, the CO_2 permeability of the neat crosslinked PEG membranes reaches 180 Barrer with high CO_2/light gas selectivity.[8] Compared with the PEG membranes formed by the classical acrylate homopolymerization, membranes prepared by using the epoxy–amine reaction exhibit around 60% higher CO_2 permeability,[13] due probably to the more flexible crosslinking network. Similarly, Patil and coworkers employed diamine JEFFAMINE and a low-molecular-weight epoxy monomer (145 g mol^{-1}) to prepare PEG-based membranes with promising CO_2 separation performance.[11] Further analysis found out that higher gas permeability can be obtained by decreasing crosslinking density (increased diffusivity), which can be accomplished by increasing the monomer length,[11,22] or adding low-molecular-weight CO_2-philic additives into the crosslinked membranes. In the first case, however, due to the highly crystalline trend between long PEG chains, the maximum monomer molecular weight is suggested to be limited within ~1000–1500 g mol^{-1}.[14,23,24] The increased monomer molecular weight seriously hinders the crosslinking reactivity, therefore higher reaction temperature or longer reaction time is required. For examples, Liu et al. used a three-stage curing method involving a precured stage at 80 °C for 3 h, followed by another 2 h at 100 °C and lastly 0.5 h at 120 °C.[8] Even with low-molecular-weight amine functionalization crosslinkers, the preparation was still complicated compared to other crosslinking mechanisms,[16,25] like the ultraviolet (UV)-induced acrylate homopolymerization.

Physically blending with low-molecular-weight additives is another widely used approach to enhance the gas transport properties of PEG-based membranes. With the presence of the liquid additives, the concentration of reactive functional groups inside monomer mixture is further diluted, which increases the difficulty to complete the reaction. To address this issue, Shao and coworkers employed a two-step method to incorporate free-PEG into the crosslinked PEG membranes, where the PEG membranes were prepared via a thermal-induced epoxy–amine reaction, then the membranes were immersed into aqueous PEG solution to obtain the PEG-imbedded membranes.[15,25] A CO_2 permeability of up to 1301 Barrer has been reported accompanied with a CO_2/H_2 selectivity of 13 after imbedding free PEG into the crosslinked PEG membranes, which makes it very promising for various CO_2 separation applications. However, the multistage membrane preparation procedure is rather time-consuming: at least 4 days was required to obtain one batch of membranes. Besides, the amount of free liquid additives inside membranes may not be controlled precisely, making it challenging for the membrane upscaling and industrial applications. Moreover, fast membrane preparation method is of great importance to promote the industrial potential of the PEG-based membranes.

Thiol–epoxy is well known for its more controllable crosslinking density, high reaction rate, and moderate reaction condition.[26,27] In this work, a one-pot synthesis method using thiol–epoxy reaction was developed to fabricate crosslinked PEG-based membranes with the presence of ionic liquids (ILs) as liquid additives. Another classical thiol-click reaction, thiol–ene, was also used to study the effects of the crosslinking reactions. ILs, the salt containing organic cation and inorganic/organic anion, which usually have a melting point lower than 100 °C, have been well accepted as membrane additives to improve the CO_2 permeation properties for their high CO_2 solubility. Various studies have incorporated highly CO_2-philic "free" ILs into polymeric membranes, and the results shows that the presence of ILs greatly enhances the CO_2 separation performance of highly crystallized polymers or crosslinked polymers, such as poly(ILs)[10,28] or PEG-based polymers.[24,29–32] In addition, the numberless combinations of various anions and cations and ILs' negligible vapor pressure offer the great opportunity for further improvement and excellent long-term stability.[33,34] Therefore, the addition of ILs was taken as an approach to improve the CO_2 permeation in the crosslinked membranes. In order to study the effect of the ILs of different anions, four ILs in a series with the same cation $[Bmim]^+$, 1-butyl-3-methylimidazolium), but different anions were selected and incorporated into the optimized crosslinked PEG-based polymeric matrix. Fourier transform infrared spectroscopy (FTIR), thermogravimetric analysis (TGA), differential scanning calorimetry (DSC), and water uptake experiments were conducted to study the chemical structure and evaluate the thermal properties and hydrophilicity of the resultant membranes. The CO_2 and N_2 transport properties of the aforementioned membranes were tested to investigate the effects of the crosslinked network structure and the addition of ILs on the CO_2 separation performance.

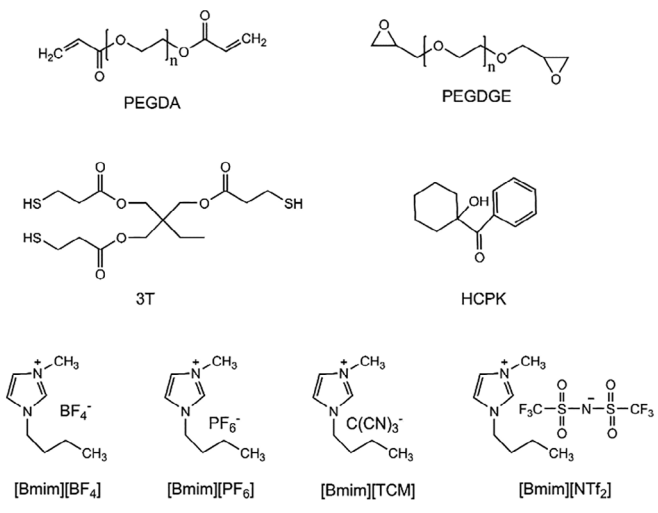

FIGURE 1 The chemical structure of PEGDA, PEGDGE 3T, and four ILs used in this work.

EXPERIMENTAL

Material

PEG diacrylate ($M_n \approx 700$) (PEGDA), trimethylolpropane tris (3-mercaptopropionate) (3T), PEG diglycidyl ether ($M_n \approx 500$) (PEGDGE), and 1-hydroxycyclohexyl phenyl ketone (HCPK) were purchased from Sigma Aldrich, Steinheim, Germany. 1-Butyl-3-methylimidazolium tetrafluoroborate ([Bmim][BF_4]), 1-butyl-3-methylimidazolium hexafluorophosphate ([Bmim][PF_6]), and 1-butyl-3-methylimidazolium bis(trifluoromethanesulfonyl)imide ([Bmim][NTf_2]) were also obtained from Sigma Aldrich. 1-Butyl-3-methylimidazolium tricyanomethanide ([Bmim][TCM]) was bought from Iolitec, Germany. The pure gases (N_2 and CO_2) used for gas separation performance evaluation were provided by AGA, Trondheim, Norway. All chemicals were used as received and their chemical structures are shown in Figure 1.

Membrane Preparation

Membranes were fabricated by a crosslinking method similar with those reported in literature[13,25] (Fig. 2). A brief description is presented below to the readers' convenience: PEGDA, PEGDGE, equivalent crosslinker 3T (mole ratio), a calculated amount of ILs, and 0.01–0.1 wt % HCPK were mixed in a glass vial for a few minutes. The content of ILs w_{IL} (%) is calculated based on the mass ratio of IL to the total membrane mass in eq 1:

$$w_{IL} = \frac{m_{IL}}{m_{PEGDGE} + m_{PEGDA} + m_{3T} + m_{IL}} \quad (1)$$

The well-mixed monomer mixture was transferred into a vacuum oven to remove the bubbles. After that, the mixture was sandwiched between two quartz plates separated by a spacer to control the thickness of membranes (~200 μm). UV irradiation with a wavelength of 365 nm (UVLS-28; Ultra-Violet Products Ltd., Cambridge, UK) was then applied to these mixture. To ensure a complete reaction, the time of UV crosslinking is set as

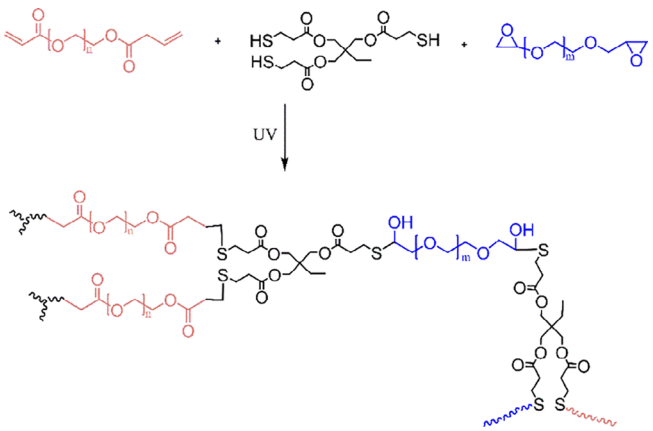

FIGURE 2 The crosslinking reactions used in this work. [Color figure can be viewed at wileyonlinelibrary.com]

1 h. The resultant self-standing membranes were obtained for further characterization and permeation test.

In this work, all membranes without ILs are systematically named according to the mole ratio between three monomers. For example, the "1–0.25–1.25" presents the membrane with 1 mol PEGDA acrylate group, 0.25 mol epoxy group and 1.25 mol thiol group, which needs 0.4745 g PEGDGE and 0.1786 g 3T per gram PEGDA. Then, 1.6531 g IL is required to prepare this membrane with 50 wt% ILs.

Characterization

A Thermo Nicolet Nexus FTIR spectrometer (NicoletTM iSTM 50; Thermo Fisher, Oslo, Norway) with a smart endurance reflection cell was used to study the chemical structure of the resultant membranes and reactants in this work. All membranes or reactants were scanned in the range of 650–4000 cm^{-1}.

Thermal stabilities of these investigated membranes were tested by a TGA (TG 209 F1 Libra; NETZSCH, Selb, Germany). Around 10–20 mg samples were used in a typical TGA test, with a temperature range of 25–700 °C and a heating rate of 10 °C min^{-1}. N_2 is employed to prevent oxidation of samples. In addition, a DSC (DSC 214 Polyma; NETZSCH) was used to investigate the glass transition temperature of the resultant membranes and reactant. Samples of around 10 mg were collected in a standard aluminum pan covered by a proper lid and heated at the rate of 10 °C min^{-1} under N_2 atmosphere.

Water uptake tests of the membrane samples were employed to evaluate the hydrophilicity of membranes. To completely remove the moisture, all membrane samples were vacuumed at 40 °C overnight. Dried samples with known weights were placed in a water desiccator at room temperature. The weights of these membrane samples were measured with a certain interval until they were stabilized. The water uptake (w_{H2O}) was calculated using eq 2:

$$w_{H2O} = \frac{w_f - w_0}{w_0} \times 100\% \quad (2)$$

where w_f and w_0 are the weight of the wet sample and dried sample, respectively.

Gas Permeation Test

Gas permeation tests were conducted at room temperature with a feed pressure of 2 bar to evaluate the CO_2 and N_2 transport properties by the constant-volume–variable-pressure method. The permeability (P) of CO_2 or N_2 was calculated by eq 3.

$$P = \left[\left(\frac{dp_d}{dt}\right)_{t\to\infty} - \left(\frac{dp_d}{dt}\right)_{leak}\right] \cdot \frac{V_d}{A \cdot R \cdot T} \cdot \frac{l}{(p_u - p_d)} \quad (3)$$

where P is the permeability, p_d and p_u represent the downstream and upstream pressure, respectively, t refers to time, V_d is the downstream volume, A means the effective permeation area of the membrane, R and T are the ideal gas constant and temperature, respectively, and l is the thickness of the membrane. The leakage rate $(dp_d/dt)_{leak}$ was measured by isolating the membrane cell at vacuum condition with air for a certain period. The thicknesses of all membranes were measured by an ABS Digimatic Indicator from Mitutoyo (Suzhou, China). The average thicknesses were given based on more than 10 measurements for each membrane. The permeability was the average values obtained based on, at least, two samples with a relative error of less than 10%. The ideal selectivity α_{CO_2/N_2} was calculated using eq 4:

$$\alpha_{CO_2/N_2} = \frac{P_{CO_2}}{P_{N_2}} \quad (4)$$

Furthermore, the diffusivity (D) was determined by the time-lag (θ) method from the single gas permeation test, and the calculation equation is shown below:

$$D = \frac{l^2}{6 \cdot \theta} \quad (5)$$

The solubility (S) was calculated by the permeability (P) and the diffusivity (D) based on the solution-diffusion mechanism:

$$S = \frac{P}{D} \quad (6)$$

RESULTS AND DISCUSSION

Membrane Preparation

Self-standing crosslinked PEGDA–PEGDGE–3T membranes were obtained after 1 h UV irradiation. The four different ILs ([Bmim][PF_6], [Bmim][TCM], [Bmim][NTf_2], and [Bmim][BF_4]) were added into the monomer mixture, and the resultant membranes were also well formed, except the one containing [Bmim][BF_4] (as shown in Fig. 3). The mixture containing [Bmim][BF_4] gels rapidly (<10 min) under atmospheric condition, even without the presence of UV or photoinitiator, suggesting that the $[BF_4]^-$ anion probably accelerates or catalyzes either thiol–ene or thiol–epoxy reaction. Since this gelation is too fast to prepare a proper membrane, the membrane containing [Bmim][BF_4] was not further characterized.

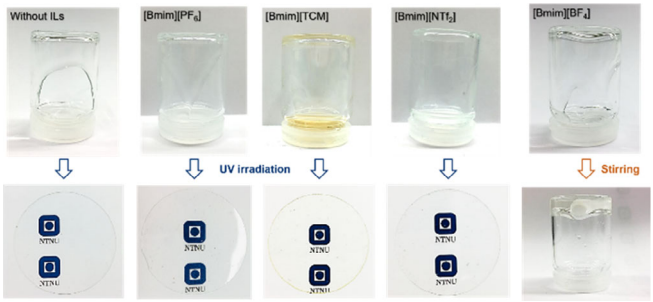

FIGURE 3 The prepolymer mixture and the formed membranes of PEGDA–PEGDGE–3T membrane (1–0.25–1.25), and the blend membranes with ILs. [Color figure can be viewed at wileyonlinelibrary.com]

Material Properties

The FTIR analysis was employed to confirm the thiol–ene and thiol–epoxy reactions between PEGDA, PEGDGE, and the crosslinker. The spectra of crosslinker, PEGDA, and the resultant membrane (1–0–1) are presented in Figure 4(A). The reactive thiol (2570 cm^{-1} for S—H) and acrylate groups (1630 cm^{-1} for C═C, 1410 and 830 cm^{-1} for H—C═) are clear in the spectra of crosslinker and PEGDA, respectively, but all of them disappear in the spectra of the resultant membranes. After the reaction, the peaks assigned to C—S bond shifts to the right side (1144–1100 cm^{-1}), which is in agreement to the literature.[35] In addition, the other peak of PEGDA at around 850 cm^{-1} becomes boarder and bigger in the resulted membranes, which may be overlapped with the peak related with the newly formed C—S bond.[36] These results suggest that the acrylate reacts with thiol and forms C—S groups under experiment conditions, confirming the completion of the thiol–ene reaction. On the other hand, in addition to the change of acrylate and thiol groups, the peak for epoxy (~904 cm^{-1}) has also disappeared in all PEGDA–PEGDGE–3T membranes, suggesting that the epoxy groups are consumed by the thiol groups, which is the only possible reactant in the system. Considering that the newly formed bonds in thiol–ene and thiol–epoxy are exactly the same, to distinguish between them via FTIR spectra is impossible and unnecessary. Hence, the membranes with different PEGDGE/PEGDA ratios have identical spectra, as present in Figure 4(C).

Since three different ILs have been embedded into the crosslinked PEG membranes, the states of ILs inside the membranes may be different, which influence the membrane properties and separation performance. The membranes with ILs were characterized by FTIR analysis, taking membranes containing 50% IL as samples, as shown in Figure 4(D). The FTIR

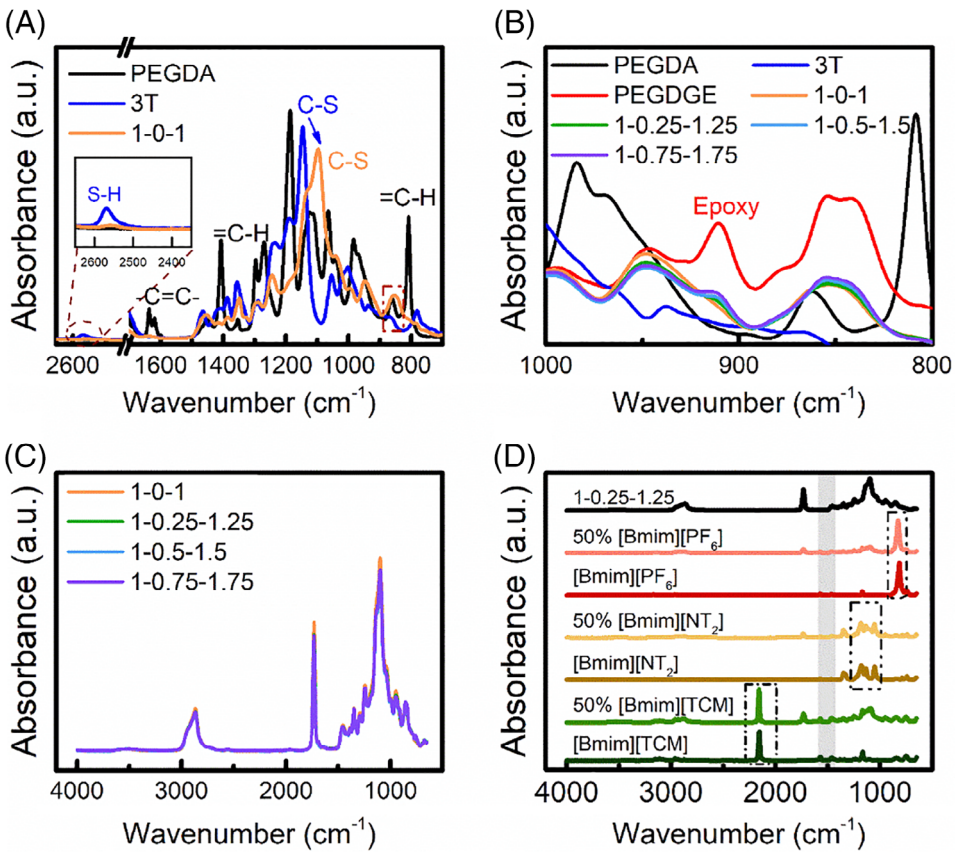

FIGURE 4 The FTIR spectrum of (A) 3T, PEGDA, and PEGDA–PEGDGE–3T (1–0–1) membranes, (B) PEGDA, PEGDGE, 3T, and PEGDA–PEGDGE–3T membranes with a different ratio at 1000–800 cm^{-1}, (C) PEGDA–PEGDGE–3T membranes with a different ratio, and (D) membrane without ILs, membrane with 50% ILs and the pure ILs. [Color figure can be viewed at wileyonlinelibrary.com]

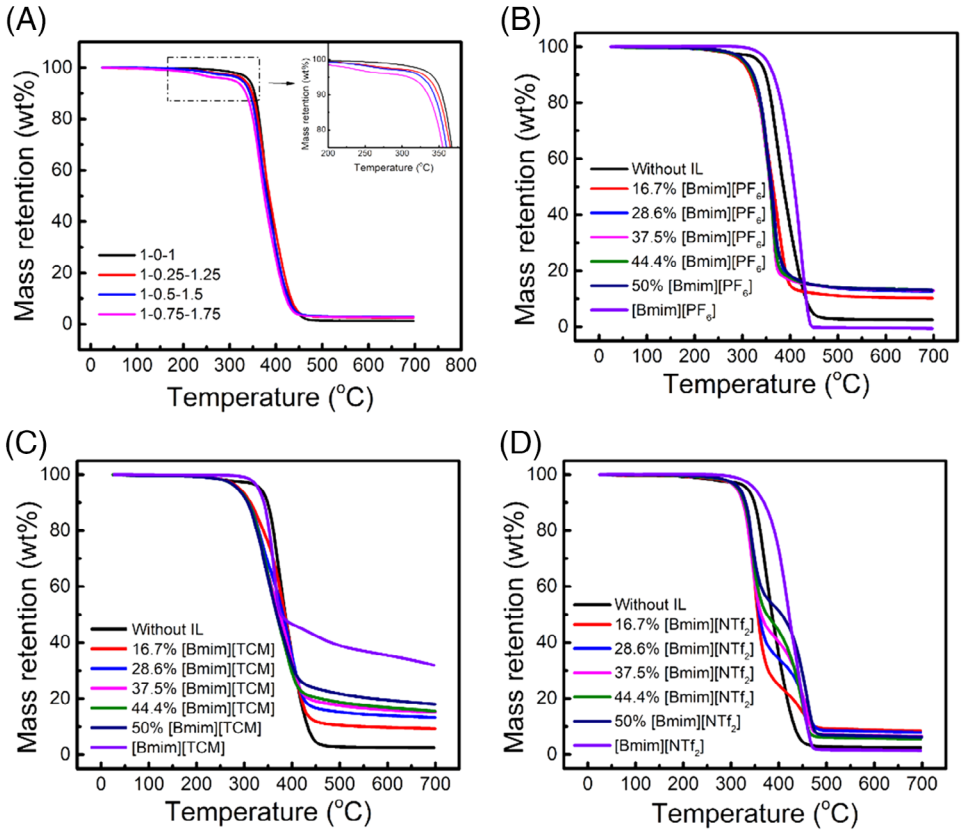

FIGURE 5 The thermal stabilities of crosslinked PEG membranes with different PEGDA/PEGDGE ratios (A), [Bmim][PF_6]-containing blend membranes (B), [Bmim][TCM]-containing blend membranes (C), and the [Bmim][NTf_2]-containing blend membranes (D) with different IL loadings. [Color figure can be viewed at wileyonlinelibrary.com]

spectra of the pristine membrane without ILs and the neat ILs are also given as a comparison. The ILs used in this work have the same cation $[Bmim]^+$, which has characteristic peaks around 1570 cm^{-1} and 1460 cm^{-1} relating to imidazolium ring.[37] These two peaks are evident in the resultant membranes with different anions. The peaks of anions are also observed in the corresponding membranes at 832 cm^{-1} (PF_6^- asymmetric stretch), 1059 cm^{-1} (S═O bending), and 1200–1130 cm^{-1} (C—F stretching) of NTf_2^-[30] and 2165 cm^{-1} of TCM^-,[38] confirming that the added ILs are embedded in the crosslinked PEG matrix. Moreover, no new peaks are found in the FTIR spectra of the blend membranes, indicating that these three ILs do not have any chemical reactions with the PEG-based monomers or the resultant polymer matrix. ILs only work as a physical additive in the investigated membranes.

The thermal stabilities of all resultant membranes in this work were studied by TGA, as shown in Figure 5. The PEGDA–3T (1–0–1) membrane shows a one-stage decomposition behavior, starting at 320 °C, while the membranes containing PEGDGE decompose at a lower temperature, and the more PEGDGE it contains, the more easily it decomposes. For the membrane containing the highest amount of PEGDGE (1–0.75–1.75), a two-stage decomposition behavior is observed; the first decomposition begins at 155 °C and the second one appears at around 300 °C, as can be seen in the insert in Figure 5(A). The weight loss during the first stage is up to 5 wt %, which may be a small amount of unreacted PEGDGE due to the less reactive thiol–epoxy under experimental conditions in this work.

The thermal stabilities of the optimized crosslinked PEG membranes (represented by 1–0.25–1.25), three IL-containing blend membranes and the corresponding ILs are displayed in Figure 5(B–D). Interestingly, although pure ILs and crosslinked PEG membranes start decomposing around 300 °C, all the blend membranes decompose at a lower temperature (around 270 °C). The reason may be ascribed to the weakened hydrogen bonding between PEG polymer chains[8,14] due to the presence of ILs inside the membranes. The [Bmim][PF_6]-containing membranes have one-stage decomposition curves, probably due to the strong interactions between [Bmim][PF_6] and polymeric matrix at high temperature conditions. Differently, the blend membranes composing [Bmim][TCM] also have similar decomposition behavior but with a slower decomposition rate, and that is because of the overlapping decomposition temperature range of their parents. On the other hand, the decomposition curves of the membrane with [Bmim][NTf_2] are close to that of [Bmim][NTf_2] at high temperature (≥430 °C), especially for those with higher IL loading, proving the existence of [Bmim][NTf_2]. These results

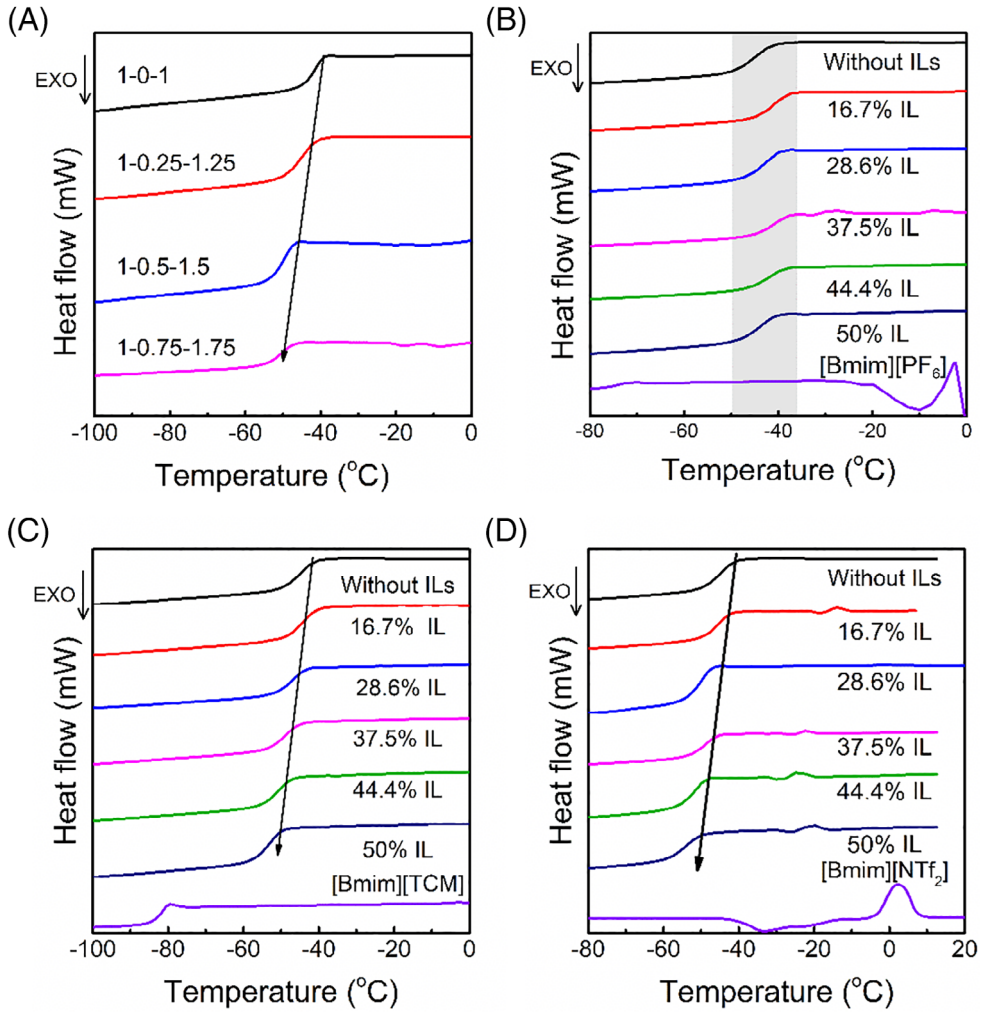

FIGURE 6 The DSC curves of crosslinked PEG membranes with different PEGDA/PEGDGE ratios (A), [Bmim][PF_6]-containing blend membranes (B), [Bmim][NTf_2]-containing blend membranes (C), and the [Bmim][TCM]-containing blend membranes (D) with different IL loadings [Color figure can be viewed at wileyonlinelibrary.com]

show that the membranes containing PEGDGE may not be suitable for a high-temperature process (≥150 °C). Generally, most CO_2 separation membrane processes are operated at a temperature range of up to 80 °C, so these resultant membranes have satisfactory thermal stabilities for this application.

As the glass transition temperature of polymers (T_g) is the temperature where polymer chains change from "restricted" to "flexible," for gas separation, a lower T_g of a membrane generally indicates a higher gas permeation property. To investigate the effects of incorporating epoxy monomers and ILs on T_g of the resultant membranes, a DSC analysis was conducted. The obtained curves are shown in Figure 6, and the T_gs are presented in Table 1.

Despite the nearly identical FTIR spectra of all the crosslinked PEGDA–PEGDGE–3T membranes, the T_gs of these membranes show a clear difference: decreasing with the increasing PEGDGE content, which implies the crosslinked network structures of these membranes may be different. As for the one containing [Bmim][PF_6], T_gs of the blend membranes show no evident difference regardless of the much lower T_g of the neat [Bmim][PF_6], which may result from the interaction of [Bmim][PF_6] with PEG-based polymer chains. Another reason may be that the presence of [Bmim][PF_6] has little effect on the T_g of matrix, and similar results have been reported in the literature.[29,39] On the other hand, the blend membranes with [Bmim][TCM] or [Bmim][NTf_2] display a decreasing trend of T_g with the increasing IL loading, possibly due to the lower value of these two ILs and the increasing chain movement with the presence of ILs. The decrease in T_g may imply an enhanced polymer chain flexibility and thus improved gas transport properties.

DSC curves can also indicate the miscibility of components in blend membranes. From Figure 6, it is clearly seen that, in the blend membranes with [Bmim][PF_6], the melting and crystallization peaks of the IL disappear, suggesting that the [Bmim][PF_6] has homogeneously dispersed within the crosslinked

TABLE 1 The T_g of Membranes Presented in Figure 6

Membranes	T_g (°C)
1–0–1	−44.7
1–0.25–1.25	−49.8
1–0.5–1.5	−53.4
1–0.75–1.75	−55.7
[Bmim][PF_6]-containing membranes	
0% [Bmim][PF_6]	−49.8
16.7% [Bmim][PF_6]	−45.5
28.6% [Bmim][PF_6]	−46.6
37.5% [Bmim][PF_6]	−45.2
44.4% [Bmim][PF_6]	−46.6
50% [Bmim][PF_6]	−48.9
Pure [Bmim][PF_6]	−75.9
[Bmim][TCM]-containing membranes	
0% [Bmim][TCM]	−49.8
16.7% [Bmim][TCM]	−48.3
28.6% [Bmim][TCM]	−51.6
37.5% [Bmim][TCM]	−53.3
44.4% [Bmim][TCM]	−55.2
50% [Bmim][TCM]	−57.6
Pure [Bmim][TCM]	−84.3
[Bmim][NTf_2]-containing membranes	
0% [Bmim][NTf_2]	−49.8
16.7% [Bmim][NTf_2]	−48.2
28.6% [Bmim][NTf_2]	−49.5
37.5% [Bmim][NTf_2]	−52.4
44.4% [Bmim][NTf_2]	−55.7
50% [Bmim][NTf_2]	−58.2
Pure [Bmim][NTf_2]	−87.5

PEG polymeric matrix. On the contrary, these peaks are visible in the DSC curves of the blend membranes containing [Bmim][NTf_2], which suggests the formation of a [Bmim][NTf_2] phase in the crosslinked PEG matrix. The hydrophobic feature of [Bmim][NTf_2] may have induced a phase separation with the hydrophilic PEG-based polymer chains as reported in the literature.[40] Nevertheless, the ILs domain regions have been reported to have a positive effect on gas transport properties[41]; hence, the crosslinked PEG membrane integrated with [Bmim][NTf_2] may still be interesting for gas separation. In the case of [Bmim][TCM], neither the melting and crystallization peaks of pure IL nor its analogy blend membranes are observed.

The water uptake experiments were conducted at room temperature for all resultant membranes. The weight gains of the membrane samples with time are presented in Figure 7. It is clear that all crosslinked PEGDA–PEGDGE–3T membranes have water uptakes of around 40 wt. %, and the PEGDGE/PEGDA ratio seems to have little effect on the material hydrophilicity. Considering that both monomers are PEG-based materials, it is reasonable to assume that the resultant networks have similar hydrophilicity.

However, the blend membranes containing different ILs present different water uptake and generally, decreases with the increasing IL amount, especially at the low IL loading range. Figure 7(B–D) presents the water uptake of various IL contents in the crosslinked membrane (1–0.25–1.25). As it can be seen, when the ILs amount is over 37.5 wt %, the water uptake is almost unchanged. Since the ILs used in this work are less hydrophilic compared with the PEG-based materials, the initial trend of declining in water uptake is expected. When the loading of ILs inside membranes increases to a certain level (>37.5 wt %), the apparent hydrophilicities of the membranes decrease to a value close to the intrinsic hydrophilicity of the ILs; hence, the water uptake of the membranes remains nearly constant with the further increase in the IL amount.

Based on the chemical structures, the hydrophilicities of the studied ILs should be different and follow the order: $TCM^- > PF_6^- > NTf_2^-$. The water uptake of the blend membranes follows the same order as the neat ILs, as can be seen in Figure 7. The [Bmim][TCM]-containing membranes have the highest water uptake of around 30 wt %, and those containing [Bmim][PF_6] have around 10 wt %, and those with the addition of [Bmim][NTf_2] present only 6 wt %. Therefore, despite the hydrophilic nature of the crosslinked PEG polymer, membranes containing the ILs become less hydrophilic.

Gas Permeation Properties

Effect of PEGDGE Addition

The CO_2 and N_2 permeation properties of the PEGDGE–PEGDA–3T membranes were tested by single gas permeation tests at a feed pressure of 2 bar and room temperature to study the effect of PEGDGE addition. The CO_2 permeability, ideal CO_2/N_2 selectivity, the gas diffusivity and solubility of the PEGDGE–PEGDA–3T membranes with different PEGDGE/PEGDA ratios are presented in Figure 8.

The CO_2 permeability increases from 100.3 to 134.2 Barrer with a nearly unchanged CO_2/N_2 selectivity of around 67 by adding a small amount of PEGDGE (1–0.25–1.25), which may be explained by the disturbance of the crosslinked PEG network due to the addition of the PEGDGE, leading to a rearranged crosslinking network and enhanced gas transport properties. The increase in diffusivities of CO_2 and N_2 [as shown in Fig. 8(B)] also suggests the increase in the free volume of the crosslinked PEG membranes. However, the CO_2 permeabilities and gas diffusivities decrease with the further increasing PEGDGE/PEGDA ratio. This trend is believed to be caused by the reduced overall chain length between the crosslinked sites since PEGDGE has shorter polymer chains (around eight EO units) compared to those of PEGDA (around 13 EO units). On the other hand, the solubility of CO_2 and N_2 in the PEGDGE–PEGDA–3T membranes is rising with the increasing PEGDGE/PEGDA ratio, which can be explained by the increased EO unit content inside these membranes. Therefore, the crosslinked networks with higher PEGDGE/PEGDA ratio become more rigid (less diffusive) with slightly increased CO_2 solubility. The CO_2/N_2 selectivity slightly

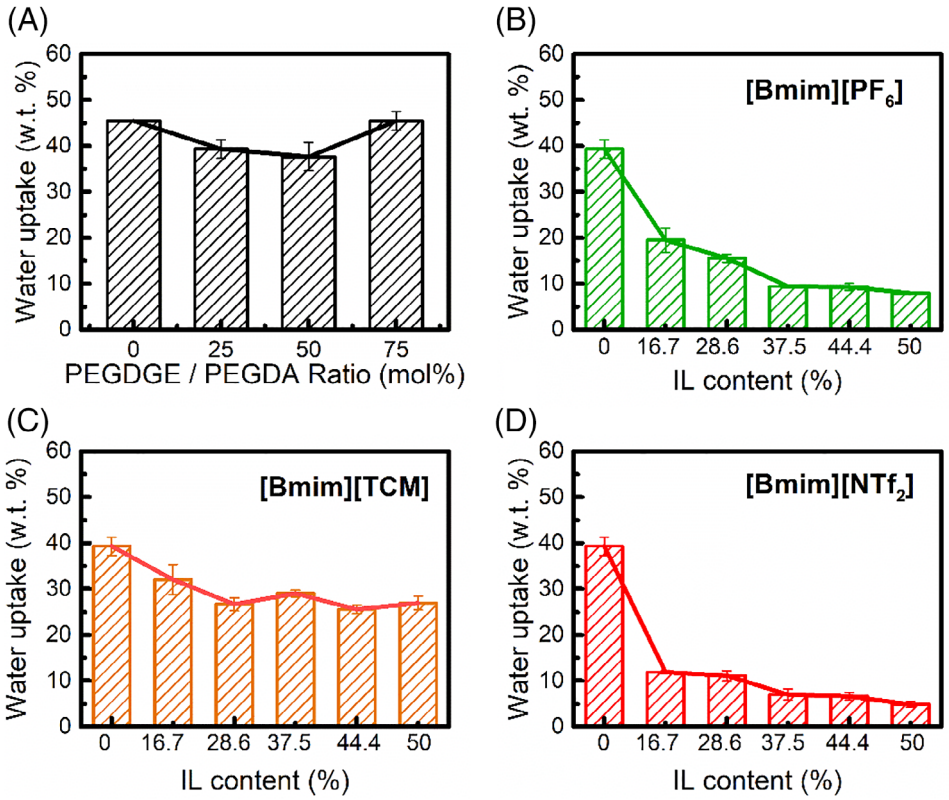

FIGURE 7 The water uptake of crosslinked PEG membranes with different PEGDA/PEGDGE ratios (A), [Bmim][PF_6]-containing blend membranes (B), [Bmim][TCM]-containing blend membranes (C), and the [Bmim][NTf_2]-containing blend membranes (D) with different IL loadings. [Color figure can be viewed at wileyonlinelibrary.com]

decreases with the increasing amount of PEGDGE in membranes, but the value (56–66) is still reasonably high and within the range of the inherent selectivity of typical PEG-based membranes.[8] Since the membrane containing the lowest amount of PEGDGE (1–0.25–1.25) holds the highest CO_2 permeability and CO_2/N_2 selectivity, it is chosen as the optimized polymeric matrix for further study.

Effects of IL Addition

Gas permeation tests of the crosslinked PEG membranes (1–0.25–1.25) containing different ILs were performed to evaluate the effects of IL addition, as presented in Figure 9. It is clearly seen that ILs with different anions show distinguishing effects on the gas permeation properties. At low IL loading (<37.5%), CO_2 permeabilities of the IL-blend membranes with [Bmim][BF_4] or [Bmim][TCM] decrease. Based on the solution-diffusion theory, the permeability is governed by diffusivity and solubility. From the diffusivity and solubility results, the reason for this drop in CO_2 permeability may be the decreased diffusivity with increasing IL loading, as it is believed that a small amount of ILs occupies the original void of the pristine polymeric membrane.[40,42] The solubility of these two series of membranes also decreases when 16.7 wt % IL is added, followed by an unaltered trend, and it may be because of the relatively lower CO_2 solubility of ILs, compared with the pure PEG-based material.[43] Interestingly, the CO_2 permeability with [Bmim][NTf_2] displays a plateau in the same IL-loading range because of the much higher CO_2 solubility, which offsets to the decrease in diffusivity. The higher CO_2 solubility could be explained by the higher CO_2 affinity of $[NTf_2]^-$ (more CO_2-philic fluorine atom) in agreement with the observation of CO_2 absorption using ILs as absorbents.[44]

At higher IL loadings, the changes in $P(CO_2)$, $D(CO_2)$, and $S(CO_2)$ of the resultant membranes containing different ILs display distinctive trends. For example, CO_2 permeability of the membranes with [Bmim][PF_6] keeps constant even at a high IL loading (i.e., 37.5–50 wt %), so do its diffusivity and solubility, suggesting that further adding [Bmim][PF_6] contributes little to these properties. On the other hand, membranes with [Bmim][TCM] or [Bmim][NTf_2] display enhanced CO_2 permeability at higher IL loading. However, the reasons responsible for these improvements are quite different: for [Bmim][TCM]-containing membranes, the increased CO_2 solubility (from 3.40×10^{-2} to 5.58×10^{-2} cm^3 (STP) cm^{-3} kPa^{-1}) is the major contributor for the gain in CO_2 permeability since the CO_2 diffusivity remains unchanged. In the case of membranes with [Bmim][NTf_2] (≥37.5 wt % IL loading), the increment in CO_2 permeability is the product of the simultaneously increased CO_2 solubility (1.90-fold) and diffusivity (3.22-fold) compared to the one containing 37.5 wt % [Bmim][NTf_2]. The increased CO_2 diffusivity is considered as

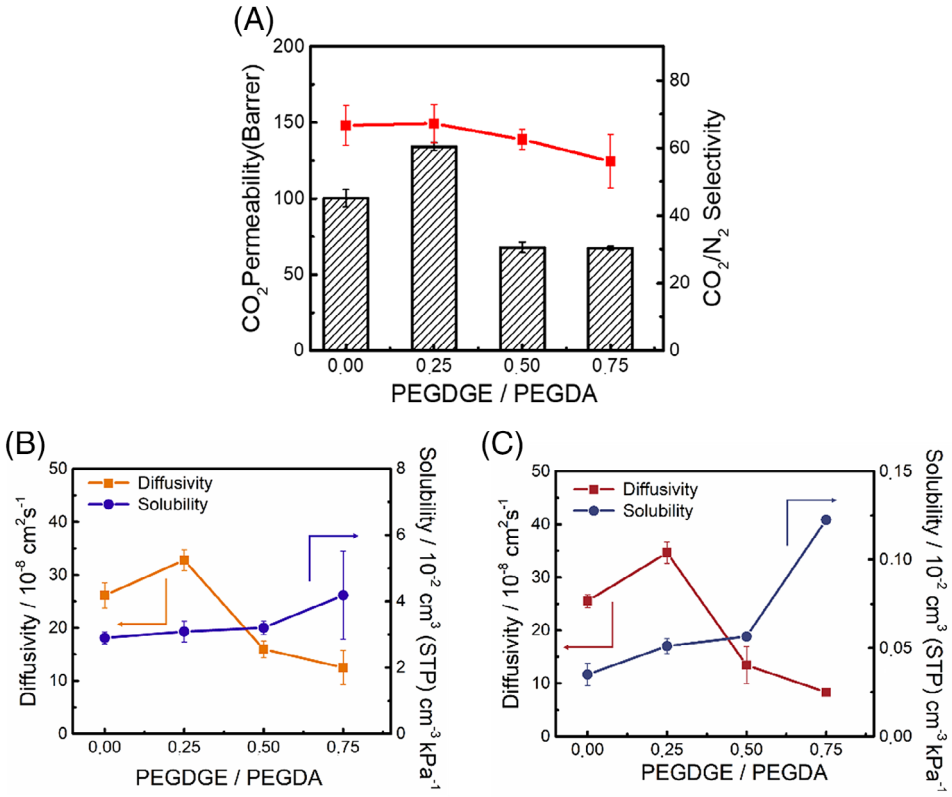

FIGURE 8 The CO_2 permeability, CO_2/N_2 selectivity (A), the diffusivity and solubility of CO_2 (B), and the diffusivity and solubility of N_2 (C) of PEGDA–PEGDGE–3T membranes with different PEGDA/PEGDGE mole ratios [Color figure can be viewed at wileyonlinelibrary.com]

the benefit of microphase separation (suggested by DSC results), leading to more IL-rich microzones and thus lower transport resistance for gas transport. As a result, the membranes with highest [Bmim][NTf_2] amount have the highest CO_2 permeability of 187.9 Barrer in this work compared to those containing [Bmim][PF_6] (53.7 Barrer) and [Bmim][TCM] (117.7 Barrer).

Hence, the change in CO_2 permeability of the blend membrane with different ILs follows different patterns. Initial adding ILs (<37.5 wt %) leads to a decrease in CO_2 diffusivity, while solubility is affected by the CO_2 affinity of ILs, and thus the resultant permeability may be decreased or unchanged. The further addition of IL shows little effect on the diffusivity, while with more additive loading, the influence of ILs on CO_2 solubility becomes the key parameter. The most CO_2-philic anion ([NTf_2]$^-$) renders the most enhanced S(CO_2), followed by the [TCM]$^-$ (due to the interaction between cyano-functionalized anion and CO_2[45]), and the [PF_6]$^-$. This order is agreed with the order of P(CO_2) and the absorption capability of these ILs for CO_2 capture.[46] It is worth mentioning that, in case of the membranes containing [Bmim][NTf_2], the microphase separation between [Bmim][NTf_2] and crosslinked PEG chains increases the D(CO_2) and thus enhances P(CO_2) more.

In terms of CO_2 selectivity, all apparent values of the membranes containing ILs are lower than the pristine one. For instance, the CO_2/N_2 selectivity of membranes with 50% IL loading are within 30–50: [Bmim][NTf_2] (34.2), [Bmim][TCM] (46.8), and [Bmim][PF_6] (38.8), while the pristine membrane has a CO_2/N_2 selectivity of 67.2. This decrease may be explained by the relatively low CO_2/N_2 selectivity of the physical-adsorption ILs (around 20–30)[43] compared with PEG-based materials (around 40–60).[8] Another possible reason is that ILs may act as the plasticizers in crosslinked PEG membranes, which could lower CO_2 selectivity.[42] In addition, different anions have distinct effects on CO_2/N_2 selectivity. Generally speaking, in this work, the order of CO_2/N_2 selectivity with a low IL amount (≤37.5%) in membranes is [PF_6]$^-$ ≈ [TMC]$^-$ > [NTf_2]$^-$, with more IL being incorporated, those containing [TMC]$^-$ move to the first in this order. The positive effects of [TMC]$^-$ on CO_2 selectivity (mainly due to the interaction between CO_2 and cyano)[41,47] are believed to be the reason of the highest value obtained in this work. The instinct of its high affinity toward CO_2 explains the excellent CO_2 selectivity in high IL loadings. [Bmim][PF_6]-containing membranes have a relatively high CO_2 selectivity, which may be because that the interaction between [PF_6]$^-$ and polymeric matrix slows down the decreasing trend of CO_2 selectivity. The data in high IL loading suggests that it may further decrease with increasing IL. On the other hand, the considerable decrease in CO_2 selectivity of [Bmim][NTf_2] could be caused by the microphase separation of IL and polymeric matrix; gas mainly passes through the IL zones, leading to the apparent selectivity close to the values of pure [Bmim][NTf_2] (around 20–30).

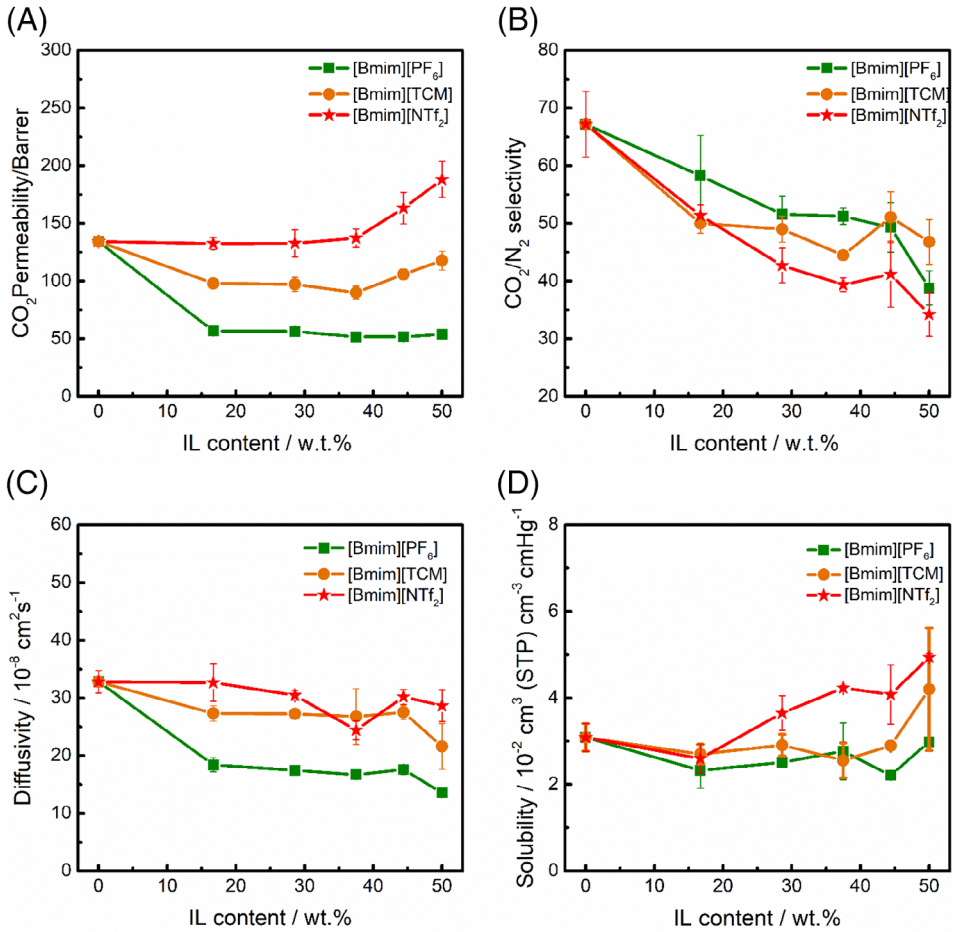

FIGURE 9 The CO_2 permeability (A), CO_2/N_2 selectivity (B), the CO_2 diffusivity (C), and CO_2 solubility (D) of three IL blend membranes with different IL loadings. [Color figure can be viewed at wileyonlinelibrary.com]

CONCLUSIONS

In the present work, crosslinked PEG-based membranes and PEG/ILs blend membranes were fabricated using one-pot thiol–ene/epoxy click chemistry. The crosslinking reactions were confirmed by FTIR analysis. The crosslinked PEG membrane was systematically evaluated using various characterization methods. The monomer ratios were optimized to enhance gas transport properties. Up to 50 wt % of ILs can be incorporated into the PEG/ILs blend membranes. The anions in ILs have significant effects on membrane structure and hence the gas separation performance. PEG membranes containing [Bmim][NTf_2] shows the highest CO_2 permeability due to the high CO_2 affinity of $[NTf_2]^-$ anion and the possible micro-separation in the membranes. On the other hand, the addition of [Bmim][TCM] is more beneficial for increasing CO_2 solubility than diffusivity, while the [Bmim][PF_6] has a negative influence on both CO_2 solubility and diffusivity.

The fabrication of the crosslinked PEG/IL membranes via the one-pot thiol–ene/epoxy click chemistry is a facile and fast method. The pairing of ILs and polymer has significant influences on the membrane material properties as well as the CO_2 separation performance. The properties of final materials are tunable by various PEG monomers and ILs, which may be practical and advantageous for feasible optimization of the blend membranes. Even the performance in this work was not greatly improved by the addition of physical-absorption ILs in this work, the addition of more CO_2-selective ILs (e.g., a chemical-absorption type of IL with CO_2/N_2 selectivity of >40) may be a promising approach worthy of further research to promote the CO_2 permeability and the selectivity of PEG-based membranes simultaneously.

ACKNOWLEDGMENT

This work is supported by the Research Council of Norway through the CLIMIT program ("POLYMEM" project, No. 254791).

CONFLICT OF INTEREST

The authors declare no conflict of interest.

REFERENCE AND NOTES

1 P. M. Lipic, F. S. Bates, M. A. Hillmyer, *J. Am. Chem. Soc.* **1998**, *120*, 8963.

2 J. Zhu, H. Q. Peng, F. Rodriguez-Macias, J. L. Margrave, V. N. Khabashesku, A. M. Imam, K. Lozano, E. V. Barrera, *Adv. Funct. Mater.* **2004**, *14*, 643.

3 A. Yamaguchi, T. Hashimoto, Y. Kakichi, M. Urushisaki, T. Sakaguchi, K. Kawabe, K. Kondo, H. Iyo, *J. Polym. Sci. Part A: Polym. Chem.* **2015**, *53*, 1052.

4 M. Furutani, A. Kakinuma, K. Arimitsu, *J. Polym. Sci. Part A: Polym. Chem.* **2018**, *56*, 237.

5 N. Makiuchi, A. Sudo, T. Endo, *J. Polym. Sci. Part A: Polym. Chem.* **2015**, *53*, 2569.

6 D. Bomze, P. Knaack, T. Koch, H. Jin, R. Liska, *J. Polym. Sci. Part A: Polym. Chem.* **2016**, *54*, 3751.

7 Y. Wang, M. Kimura, A. Sudo, T. Endo, *J. Polym. Sci. Part A: Polym. Chem.* **2016**, *54*, 2611.

8 S. L. Liu, L. Shao, M. L. Chua, C. H. Lau, H. Wang, S. Quan, *Prog. Polym. Sci.* **2013**, *38*, 1089.

9 W. M. McDanel, M. G. Cowan, N. O. Chisholm, D. L. Gin, R. D. Noble, *J. Membr. Sci.* **2015**, *492*, 303.

10 W. M. McDanel, M. G. Cowan, T. K. Carlisle, A. K. Swanson, R. D. Noble, D. L. Gin, *Polymer* **2014**, *55*, 3305.

11 P. N. Patil, D. Roilo, R. S. Brusa, A. Miotello, R. Checchetto, *Polymer* **2015**, *58*, 130.

12 L. M. Robeson, *J. Membr. Sci.* **2008**, *320*, 390.

13 H. Lin, B. D. Freeman, *Macromolecules* **2005**, *38*, 8394.

14 J. Liu, X. Hou, H. B. Park, H. Lin, *Chem. Eur. J.* **2016**, *22*, 15980.

15 S. Quan, Y. P. Tang, Z. X. Wang, Z. X. Jiang, R. G. Wang, Y. Y. Liu, L. Shao, *Macromol. Rapid Commun.* **2015**, *36*, 490.

16 S. Quan, S. Li, Z. Wang, X. Yan, Z. Guo, L. Shao, *J. Mater. Chem. A* **2015**, *3*, 13758.

17 S. Li, X. Jiang, Q. Yang, L. Shao, *Chem. Eng. Res. Des.* **2017**, *122*, 280.

18 S. Quan, S. W. Li, Y. C. Xiao, L. Shao, *Int. J. Greenh. Gas Con.* **2017**, *56*, 22.

19 X. Jiang, S. Li, S. He, Y. Bai, L. Shao, *J. Mater. Chem. A* **2018**, *6*, 15064.

20 S. Li, X. Jiang, X. Yang, Y. Bai, L. Shao, *J. Membr. Sci.* **2019**, *570–571*, 278.

21 X. Jiang, S. He, S. Li, Y. Bai, L. Shao, *J. Mater. Chem. A* **2019**, *7*, 16704.

22 D. Roilo, P. N. Patil, R. S. Brusa, A. Miotello, R. Checchetto, *Polymer* **2017**, *113*, 147.

23 N. P. Patel, A. C. Miller, R. Spontak, *J. Adv. Funct. Mater.* **2004**, *14*, 699.

24 J. Deng, J. Yu, Z. Dai, L. Deng, *Ind. Eng. Chem. Res.* **2019**, *58*, 5261.

25 Z. Dai, L. Ansaloni, D. L. Gin, R. D. Noble, L. Deng, *J. Membr. Sci.* **2017**, *523*, 551.

26 C. E. Hoyle, A. B. Lowe, C. N. Bowman, *Chem. Soc. Rev.* **2010**, *39*, 1355.

27 K. Jin, N. Wilmot, W. H. Heath, J. M. Torkelson, *Macromolecules* **2016**, *49*, 4115.

28 J. E. Bara, D. L. Gin, R. D. Noble, *Ind. Eng. Chem. Res.* **2008**, *47*, 9919.

29 Z. Dai, L. Bai, K. N. Hval, X. Zhang, S. Zhang, L. Deng, *Sci. China. Chem.* **2016**, *59*, 538.

30 M. Li, X. Zhang, S. Zeng, H. Gao, J. Deng, Q. Yang, S. Zhang, *RSC Adv.* **2017**, *7*, 6422.

31 W. Fam, J. Mansouri, H. Li, V. Chen, *J. Membr. Sci.* **2017**, *537*, 54.

32 V. A. Kusuma, M. K. Macala, J. Liu, A. M. Marti, R. J. Hirsch, L. J. Hill, D. Hopkinson, *J. Membr. Sci.* **2018**, *545*, 292.

33 K. Fujii, T. Makino, K. Hashimoto, T. Sakai, M. Kanakubo, M. Shibayama, *Chem. Lett.* **2014**, *44*, 17.

34 M. Karunakaran, L. F. Villalobos, M. Kumar, R. Shevate, F. H. Akhtar, K.-V. Peinemann, *J. Mater. Chem. A* **2017**, *5*, 649.

35 Y. Zhao, X. Zhang, Y. He, N. Liu, T. Tan, C. Liang, *Materials* **2017**, *10*, 1158.

36 B. Wei, L. Ouyang, J. Liu, D. C. Martin, *J. Mater. Chem. B* **2015**, *3*, 5028.

37 J. Im, S. D. Cho, M. H. Kim, Y. M. Jung, H. S. Kim, H. S. Park, *Chem. Commun.* **2012**, *48*, 2015.

38 D. G. Kuroda, P. K. Singh, R. M. Hochstrasser, *J. Phys. Chem. B* **2012**, *117*, 4354.

39 A. Ito, T. Yasuda, X. Ma, M. Watanabe, *Polym. J.* **2017**, *49*, 671.

40 P. Bernardo, J. C. Jansen, F. Bazzarelli, F. Tasselli, A. Fuoco, K. Friess, P. Izák, V. Jarmarová, M. Kačírková, G. Clarizia, *Sep. Purif. Technol.* **2012**, *97*, 73.

41 H. Z. Chen, P. Li, T.-S. Chung, *Int. J. Hydrogen Energy* **2012**, *37*, 11796.

42 S. Kanehashi, M. Kishida, T. Kidesaki, R. Shindo, S. Sato, T. Miyakoshi, K. Nagai, *J. Membr. Sci.* **2013**, *430*, 211.

43 Z. Dai, R. D. Noble, D. L. Gin, X. Zhang, L. Deng, *J. Membr. Sci.* **2016**, *497*, 1.

44 S. Zeng, X. Zhang, L. Bai, X. Zhang, H. Wang, J. Wang, D. Bao, M. Li, X. Liu, S. Zhang, *Chem. Rev.* **2017**, *117*, 9625.

45 L. C. Tomé, I. M. Marrucho, *Chem. Soc. Rev.* **2016**, *45*, 2785.

46 Z. Lei, C. Dai, B. Chen, *Chem. Rev.* **2013**, *114*, 1289.

47 L. C. Tomé, M. Isik, C. S. Freire, D. Mecerreyes, I. M. Marrucho, *J. Membr. Sci.* **2015**, *483*, 155.